3 Astrophysical Axion Bounds

Georg G. Raffelt

Max-Planck-Institut für Physik (Werner-Heisenberg-Institut), Föhringer Ring 6, 80805 München, Germany
raffelt@mppmu.mpg.de

Abstract. Axion emission by hot and dense plasmas is a new energy-loss channel for stars. Observable consequences include a modification of the solar sound-speed profile, an increase of the solar neutrino flux, a reduction of the helium-burning lifetime of globular-cluster stars, accelerated white-dwarf cooling, and a reduction of the supernova SN 1987A neutrino burst duration. I review and update these arguments and summarize the resulting axion constraints.

3.1 Introduction

The "outer space" of astrophysics and cosmology provides a natural laboratory for the "inner space" of elementary particle physics. Usually, one may first think of the early universe or perhaps high-energy cosmic rays for arguments in favor of or against a new particle-physics model. However, in the case of axions, the low energies available in stars are well suited for very sensitive tests.

The basic idea is very simple. Stars are powerful sources of weakly interacting particles such as neutrinos, gravitons, hypothetical axions, and other new particles that can be produced by nuclear reactions or by thermal processes in the stellar interior. Even when this particle flux cannot be directly measured, the properties of stars themselves would change if they lost too much energy into a new channel. This "energy-loss argument" has been widely used to constrain a long list of particle properties; see [1, 2, 3, 4, 5, 6, 7] for early examples and [8, 9, 10, 11, 12] for extensive reviews. I summarize here the main arguments that have been put forward, the observational evidence, and the resulting constraints for "invisible axions".

To this end, I review in Sect. 3.2 the axion interactions with photons and fermions. In Sect. 3.3, I consider the Sun as an axion source, notably by the Primakoff process, and review limits on the axion-photon interaction strength by helioseismology, the measured neutrino flux, and the CAST experiment. In Sects. 3.4, 3.5, and 3.6, I review axion limits from globular-cluster stars, white-dwarf cooling, and supernova SN 1987A, respectively. I summarize these constraints in Sect. 3.7 in juxtaposition with cosmological arguments.

G.G. Raffelt: *Astrophysical Axion Bounds*, Lect. Notes Phys. **741**, 51–71 (2008)
DOI 10.1007/978-3-540-73518-2_3

3.2 Axion Interactions

The particle-physics motivation for "invisible" axions and their main properties were introduced in Chap. 1 of this volume. Before turning to their role in stars, we briefly review the phenomenological properties of these pseudo Nambu-Goldstone bosons of the Peccei-Quinn (PQ) symmetry. The mass and interaction strength with ordinary particles are approximately given in terms of the relevant π^0 properties, scaled with f_π/f_a where $f_\pi = 92\,\mathrm{MeV}$ is the pion decay constant and f_a is the PQ scale or axion decay constant. The normalization of f_a is defined by the axion-gluon interaction

$$L_{a\gamma\gamma} = \frac{g_{\rm s}^2}{32\,\pi^2}\,\frac{a}{f_a}\,G^b_{\mu\nu}\tilde{G}^{b\mu\nu}\ , \tag{3.1}$$

where a is the axion field, G the gluon field-strength tensor, $\tilde{G}$ its dual, and b a color index. Color anomaly factors have been absorbed in this definition of f_a, which is the quantity that is relevant for all low-energy phenomena [13].

The PQ symmetry is explicitly broken at low energies and axions acquire a small mass. Unless there are non-QCD contributions, perhaps from Planck-scale physics [14, 15], the mass is

$$m_a = \frac{z^{1/2}}{1+z}\,\frac{f_\pi m_\pi}{f_a} = \frac{6.0\,\mathrm{eV}}{f_a/10^6\,\mathrm{GeV}}\ , \tag{3.2}$$

where $z = m_u/m_d$ is the up/down quark mass ratio. We will follow the previous axion literature and usually assume the canonical value $z = 0.56$ [16, 17], although it could vary in the range $z = 0.3$–0.6 [12].

Another generic property of axions is their two-photon interaction that plays a key role for most searches,

$$L_{a\gamma\gamma} = \frac{g_{a\gamma\gamma}}{4}\,F_{\mu\nu}\tilde{F}^{\mu\nu}a = -g_{a\gamma\gamma}\,\mathbf{E}\cdot\mathbf{B}\,a\ . \tag{3.3}$$

Here, F is the electromagnetic field-strength tensor, $\tilde{F}$ its dual, and $\mathbf{E}$ and $\mathbf{B}$ the electric and magnetic fields, respectively. The coupling constant is

$$g_{a\gamma\gamma} = \frac{\alpha}{2\pi f_a}\left(\frac{E}{N} - \frac{2}{3}\,\frac{4+z}{1+z}\right) = \frac{\alpha}{2\pi}\left(\frac{E}{N} - \frac{2}{3}\,\frac{4+z}{1+z}\right)\frac{1+z}{z^{1/2}}\,\frac{m_a}{m_\pi f_\pi}\ , \tag{3.4}$$

where E and N, respectively, are the electromagnetic and color anomaly of the axial current associated with the axion field. $E/N = 0$ in the Kim-Shifman-Vainshtein-Zakharov (KSVZ) model [18, 19], whereas $E/N = 8/3$ in grand unified models, e.g., the Dine-Fischler-Srednicki-Zhitnitskii (DFSZ) model [20, 21]. While these cases are often used as generic examples, in general E/N is not known so that for fixed f_a a broad range of $g_{a\gamma\gamma}$ values is possible [22]. Still, barring fine-tuned cancelations, $g_{a\gamma\gamma}$ scales from the corresponding pion interaction by virtue of the relation (3.4). Taking the

model-dependent factors to be of order unity, this relation defines the "axion line" in the m_a–$g_{a\gamma\gamma}$ plane.

Axions or axion-like particles with a two-photon vertex decay into two photons with a rate

$$\begin{aligned}\Gamma_{a\to\gamma\gamma} &= \frac{g_{a\gamma\gamma}^2 m_a^3}{64\,\pi} = \frac{\alpha^2}{256\,\pi^3}\left[\left(\frac{E}{N}-\frac{2}{3}\,\frac{4+z}{1+z}\right)\frac{1+z}{z^{1/2}}\right]^2 \frac{m_a^5}{m_\pi^2 f_\pi^2} \\ &= 1.1\times 10^{-24}\,\mathrm{s}^{-1}\left(\frac{m_a}{\mathrm{eV}}\right)^5, \end{aligned} \tag{3.5}$$

where the first expression is for general pseudoscalars, the second applies specifically to axions, and the numerical one assumes $z = 0.56$ and the hadronic case $E/N = 0$. Comparison with the age of the universe of $4.3\times 10^{17}\,\mathrm{s}$ reveals that axions decay on a cosmic time scale if $m_a \gtrsim 20\,\mathrm{eV}$.

The interaction with fermions j has a derivative structure so that it is invariant under $a \to a + a_0$ as behooves a Nambu-Goldstone boson,

$$L_{ajj} = \frac{C_j}{2f_a}\,\bar\Psi_j\gamma^\mu\gamma_5\Psi_j\partial_\mu a \quad \text{or} \quad -\mathrm{i}\,\frac{C_j m_j}{f_a}\,\bar\Psi_j\gamma_5\Psi_j a\,. \tag{3.6}$$

Here, Ψ_j is the fermion field, m_j its mass, and C_j a model-dependent numerical coefficient. The combination $g_{ajj} \equiv C_j m_j/f_a$ plays the role of a Yukawa coupling and $\alpha_{ajj} \equiv g_{ajj}^2/4\pi$ that of a "fine-structure constant". The pseudoscalar form is usually equivalent to the derivative structure, but one has to be careful in processes where two Nambu-Goldstone bosons are attached to one fermion line, for example, an axion and a pion attached to a nucleon in the context of axion emission by nucleon bremsstrahlung [23, 24].

In hadronic models such as KSVZ [18, 19], axions do not couple to ordinary quarks and leptons at tree level, whereas in the DFSZ model [20, 21]

$$C_e = \frac{\cos^2\beta}{3}\,. \tag{3.7}$$

Here, $\cot\beta$ is the ratio of two Higgs vacuum expectation values of this model.

For nucleons, the dimensionless couplings $C_{n,p}$ are related by generalized Goldberger-Treiman relations to nucleon axial-vector current matrix elements,

$$\begin{aligned} C_p &= (C_u-\eta)\,\Delta u + (C_d-\eta z)\,\Delta\mathrm{d} + (C_s-\eta w)\,\Delta s\,, \\ C_n &= (C_u-\eta)\,\Delta\mathrm{d} + (C_d-\eta z)\,\Delta u + (C_s-\eta w)\,\Delta s\,. \end{aligned} \tag{3.8}$$

Here, $\eta = (1+z+w)^{-1}$ with $z = m_u/m_d$ and $w = m_u/m_s \ll z$. The quantities Δq represent the axial-vector current couplings to the proton, $\Delta q\,S_\mu = \langle p|\bar q\gamma_\mu\gamma_5 q|p\rangle$ where S_μ is the proton spin.

Neutron beta decay and strong isospin symmetry tell us that $\Delta u - \Delta\mathrm{d} = F + D = 1.267 \pm 0.0035$, whereas hyperon decays and flavor SU(3) symmetry imply $\Delta u + \Delta\mathrm{d} - 2\Delta s = 3F - D = 0.585 \pm 0.025$. Recent determinations

of the strange-quark contribution are $\Delta s = -0.08 \pm 0.01_{\rm stat} \pm 0.05_{\rm syst}$ from the COMPASS experiment [25] and $\Delta s = -0.085 \pm 0.008_{\rm exp} \pm 0.013_{\rm theor} \pm 0.009_{\rm evol}$ from HERMES [26], in agreement with each other and with an early estimate of $\Delta s = -0.11 \pm 0.03$ [27]. We thus adopt the estimates

$$\begin{aligned} \Delta u &= +0.841 \pm 0.020\,, \\ \Delta {\rm d} &= -0.426 \pm 0.020\,, \\ \Delta s &= -0.085 \pm 0.015\,, \end{aligned} \tag{3.9}$$

that are very similar to previous values used in the axion literature.

The uncertainty of the axion-nucleon couplings is dominated by the large uncertainty of $z = 0.3$–0.6 that was mentioned above. For hadronic axions we have $C_{u,d,s} = 0$ so that $C_p = -0.55$ and $C_n = +0.14$ for $z = 0.3$ and $C_p = -0.37$ and $C_n = -0.05$ for $z = 0.6$. Therefore, while it is well possible that $C_n = 0$, C_p does not vanish within the plausible z range. In the DFSZ model we have $C_u = \frac{1}{3}\sin^2\beta$ and $C_d = \frac{1}{3}\cos^2\beta$. Even with the large allowed z range, C_n and C_p never vanish simultaneously. An extreme case is $\cos^2\beta = 0$ where $C_p = 0$ for $z = 0.3$, but in this case $C_n = -0.27$.

3.3 The Sun as an Axion Source

3.3.1 Axion Flux from the Primakoff Process

The Sun would be a powerful axion source. This flux can be searched directly, notably by the CAST experiment. Its sensitivity is competitive with the globular-cluster limits (Sect. 3.4) for hadronic models. In this case, the dominant emission process is the Primakoff effect [28], i.e., particles with a two-photon vertex transform into photons in external electric or magnetic fields. Therefore, stars produce axions from thermal photons in the fluctuating electromagnetic fields of the stellar plasma [6].

Calculating the solar axion flux is straightforward except for the proper inclusion of screening effects [29, 30]. The transition rate for a photon of energy E into an axion of the same energy (recoil effects are neglected) [31] is

$$\Gamma_{\gamma\to a} = \frac{g_{a\gamma\gamma}^2 T \kappa_{\rm s}^2}{32\pi}\left[\left(1+\frac{\kappa_{\rm s}^2}{4E^2}\right)\ln\left(1+\frac{4E^2}{\kappa_{\rm s}^2}\right)-1\right], \tag{3.10}$$

where T is the temperature (natural units with $\hbar = c = k_{\rm B} = 1$ are used). The screening scale in the Debye-Hückel approximation is

$$\kappa_{\rm s}^2 = \frac{4\pi\alpha}{T}\left(n_e + \sum_{\rm nuclei} Z_j^2 n_j\right), \tag{3.11}$$

where n_e is the electron density and n_j the density of the j-th ion of charge Z_j. Near the solar center $\kappa_{\rm s} \approx 9\,{\rm keV}$. Note that $(\kappa_{\rm s}/T)^2 \approx 12$ is nearly

constant throughout the Sun whereas it is about 2.5 throughout the core of a low-mass helium-burning star.

Ignoring the plasma frequency for the initial-state photons, the energy-loss rate per unit volume is [10, 31]

$$Q = \frac{g_{a\gamma\gamma}^2 T^7}{4\pi} F \,, \tag{3.12}$$

where F is a numerical factor of order unity. For $(\kappa_s/T)^2 = 2.5$ and 12 one finds $F = 0.98$ and 1.84, respectively.

Integrating over a standard solar model, one finds an axion flux at Earth that is well approximated by (E in keV)

$$\frac{\mathrm{d}\Phi_a}{\mathrm{d}E} = g_{10}^2 \; 6.0 \times 10^{10}\,\mathrm{cm}^{-2}\,\mathrm{s}^{-1}\,\mathrm{keV}^{-1}\,E^{2.481}\,\mathrm{e}^{-E/1.205} \,, \tag{3.13}$$

where $g_{10} = g_{a\gamma\gamma}/(10^{-10}\,\mathrm{GeV}^{-1})$. The integrated flux parameters are

$$\begin{aligned} \Phi_a &= g_{10}^2\, 3.75 \times 10^{11}\,\mathrm{cm}^{-2}\,\mathrm{s}^{-1} \,, \\ L_a &= g_{10}^2\, 1.85 \times 10^{-3} L_\odot \,. \end{aligned} \tag{3.14}$$

The maximum of the distribution is at 3.0 keV, and the average energy is 4.2 keV.

3.3.2 Solar Age

The properties of the Sun itself constrain this flux. The axion losses lead to an enhanced consumption of nuclear fuel. The standard Sun is halfway through its hydrogen-burning phase so that the solar axion luminosity should not exceed its photon luminosity $L_\odot$.

As an example let us recall that a magnetically-induced vacuum dichroism observed by the PVLAS experiment [32], if interpreted in terms of an axion-like particle (ALP), requires [32, 33] $g_{a\gamma\gamma} = 2\text{–}5 \times 10^{-6}\,\mathrm{GeV}^{-1}$ and $m_a = 1\text{–}1.5\,\mathrm{meV}$. With this coupling strength, the Sun's ALP luminosity would exceed $L_\odot$ by a factor of a million and thus it could live only for about 1000 years. Perhaps this problem can be circumvented, but it is noteworthy that even a crude astrophysical argument severely constrains the particle interpretation of the PVLAS signature.

3.3.3 Helioseismology

For a more refined constraint, we note that a model of the present-day Sun, with the integrated effect of axion losses taken into account, would differ from a standard solar model. The modified sound-speed profile can be diagnosed by helioseismology, providing a conservative limit [34]

$$g_{a\gamma\gamma} \lesssim 1 \times 10^{-9}\,\mathrm{GeV}^{-1}\,, \tag{3.15}$$

corresponding to $L_a \lesssim 0.20\,L_\odot$. More recent determinations of the solar metal abundances have diminished the agreement between standard solar models and helioseismology [35], but these modifications do not change the limit (3.15).

3.3.4 Solar Neutrino Flux

The energy loss by solar axion emission requires enhanced nuclear burning and thus a somewhat increased temperature in the Sun. Self-consistent solar models with axion losses reveal that $g_{a\gamma\gamma} = 4.5 \times 10^{-10}\,\mathrm{GeV}^{-1}$ implies a 20% increase of the solar ^{8}B neutrino flux [34]. For $g_{a\gamma\gamma} = 10 \times 10^{-10}\,\mathrm{GeV}^{-1}$ the increase would be a factor of 2.4.

The measured all-flavor ^{8}B neutrino flux is $4.94 \times 10^6\,\mathrm{cm}^{-2}\,\mathrm{s}^{-1}$ with an uncertainty of about 8.8% [36, 37]. The old standard solar model predictions were about 5.7–5.9 in the same units, whereas the new metal abundances imply 4.5–4.6, each time with a 16% "theoretical 1σ error" [35]. Therefore, the measured neutrino fluxes imply a limit

$$g_{a\gamma\gamma} \lesssim 5 \times 10^{-10}\,\mathrm{GeV}^{-1}\,, \tag{3.16}$$

corresponding to $L_a \lesssim 0.04\,L_\odot$. A more precise limit with a realistic error budget would require self-consistent solar models on a finer spacing of $g_{a\gamma\gamma}$.

3.3.5 Searches for Solar Axions

The solar axion flux can be searched with the inverse Primakoff process where axions convert to photons in a macroscopic B field, the "axion helioscope" technique [38]. One would look at the Sun through a "magnetic telescope" and place an X-ray detector at the far end. The conversion can be coherent over a large propagation distance and is then pictured as a particle oscillation effect [39].

Early helioscope searches were performed in Brookhaven [40] and Tokyo [41, 42]. Solar axions could also transform in electric crystal fields, but the limits obtained by SOLAX [43], COSME [44], and DAMA [45] are less restrictive and require a solar axion luminosity exceeding (3.15) and (3.16), i.e., these limits are not self-consistent.

The first helioscope that can actually reach the "axion line" is the CERN Axion Solar Telescope (CAST). The non-observation of a signal above background leads to a constraint [46]

$$g_{a\gamma\gamma} < 1.16 \times 10^{-10}\,\mathrm{GeV}^{-1} \quad (95\%\ \mathrm{CL}) \qquad \text{for} \quad m_a \lesssim 0.02\,\mathrm{eV}\,. \tag{3.17}$$

For larger masses, the axion-photon transition is suppressed by the energy-momentum mismatch between particles of different mass. The full rate can

be restored in a narrow range of masses by providing the photons with a refractive mass in the presence of a low-Z gas [47], a method that was already used in the Tokyo experiment [42] and is also used in the ongoing CAST Phase II. CAST is foreseen to reach eventually $m_a \lesssim 1\,\mathrm{eV}$.

3.3.6 Do Axions Escape from the Sun?

CAST can detect axions only if they actually escape from the Sun. Their mean free path (mfp) against the Primakoff process is the inverse of (3.10). For 4 keV axions with $T \approx 1.3\,\mathrm{keV}$ and $\kappa_\mathrm{s} \approx 9\,\mathrm{keV}$ at the solar center we find $\lambda_a \approx g_{10}^{-2}\, 6 \times 10^{24}\,\mathrm{cm} \approx g_{10}^{-2}\, 8 \times 10^{13}\, R_\odot$ or about 10^{-3} of the radius of the visible universe. Therefore, $g_{a\gamma\gamma}$ would have to be more than 10^7 times larger than the CAST limit for axions to be re-absorbed in the Sun.

Even in this extreme case they are not harmless because they would carry the bulk of the energy flux that otherwise is carried by photons. The mfp of low-mass particles in the trapping regime should be shorter than that of photons (about 10 cm near the solar center) to avoid a dramatic modification of the solar structure [48]. This requirement is so extreme that for anything similar to axions, the possibility of re-absorption is not a serious possibility.

3.4 Globular-Cluster Stars

3.4.1 Helium-Burning Lifetime and the Axion-Photon Interaction

A restrictive limit on $g_{a\gamma\gamma}$ arises from globular-cluster stars. A globular cluster is a gravitationally bound system of stars that formed at the same time and thus differ primarily in their mass. A globular cluster provides a homogeneous population of stars, allowing for detailed tests of stellar-evolution theory. The stars surviving since formation have masses somewhat below $1\,M_\odot$. In a color-magnitude diagram (Fig. 3.1), where one plots essentially the surface brightness vs. the surface temperature, stars appear in characteristic loci, allowing one to identify their state of evolution.

The stars on the horizontal branch (HB) have reached helium burning, where their core (about $0.5\,M_\odot$) generates energy by fusing helium to carbon and oxygen with a core-averaged energy release of about $80\,\mathrm{erg\,g^{-1}\,s^{-1}}$. A typical density is $10^4\,\mathrm{g\,cm^{-3}}$, and a typical temperature $10^8\,\mathrm{K}$. The Primakoff energy-loss rate (3.12) implies that the energy-loss rate per unit mass, $\varepsilon = Q/\varrho$, is proportional to T^7/ϱ. Averaged over a typical HB-star core one finds $\langle (T/10^8\,\mathrm{K})^7\,(10^4\,\mathrm{g\,cm^{-3}}/\varrho)\rangle \approx 0.3$. Therfore, the core-averaged energy-loss rate is about $g_{10}^2\,30\,\mathrm{erg\,g^{-1}\,s^{-1}}$. The main effect would be accelerated consumption of helium and thus a reduction of the HB lifetime by a factor $80/(80 + 30\,g_{10}^2)$, i.e., by about 30% for $g_{10} = 1$.

The HB lifetime can be measured relative to the red-giant evolutionary time scale by comparing the number of HB stars with the number of RGB

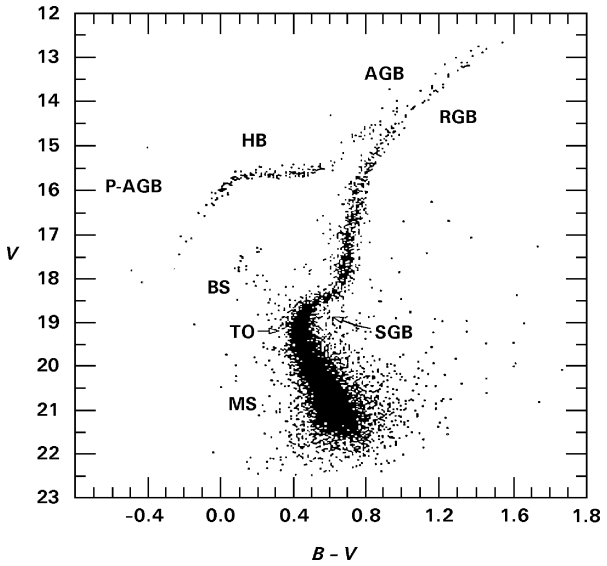

Fig. 3.1. Color-magnitude diagram for the globular cluster M3, based on 10,637 stars [50]. Vertically is the brightness in the visual (V) band, horizontally the difference between B (blue) and V brightness, i.e., a measure of the color and thus surface temperature, where blue (hot) stars lie toward the left. The classification for the evolutionary phases is as follows [51]. MS (main sequence): core hydrogen burning. BS (blue stragglers). TO (main-sequence turnoff): central hydrogen is exhausted. SGB (subgiant branch): hydrogen burning in a thick shell. RGB (red-giant branch): hydrogen burning in a thin shell with a growing core until helium ignites. HB (horizontal branch): helium burning in the core and hydrogen burning in a shell. AGB (asymptotic giant branch): helium and hydrogen shell burning. P-AGB (post-asymptotic giant branch): final evolution from the AGB to the white-dwarf stage

stars that are brighter than the HB. Number counts in 15 globular clusters [49] show that this number ratio agrees with expectations within 20–40% in any one cluster, where the error is mostly statistical because typically only about 100 HB stars were present in the fields of view used. Compounding the results of all 15 clusters, the helium-burning lifetime agrees with expectations within about 10% [10, 11]. Of course, with modern data these results could likely be improved. Either way, a reasonably conservative limit is

$$g_{a\gamma\gamma} < 10^{-10}\,\mathrm{GeV}^{-1}\,. \tag{3.18}$$

It is comparable to the CAST limit (3.17), but applies for higher masses. The relevant temperature is about 10 keV so that significant threshold effects begin only at about $m_a \gtrsim 30\,\mathrm{keV}$. For QCD axions, the coupling increases with mass so that the limit applies to even larger masses.

In the helium-burning core, convection and semi-convection dredges helium to the burning site so that 25–30% of all helium is burnt during the HB phase. Therefore, while the standard theoretical predictions depend on a phenomenological treatment of convection, there is limited room for additional energy supply, even if the treatment of convection were grossly incorrect.

3.4.2 Helium Ignition and the Axion-Electron Interaction

RGB stars have a degenerate helium core with a typical density $10^6\,\mathrm{g\,cm^{-3}}$ and $T \approx 10^8\,\mathrm{K}$. Helium ignites at a critical combination of ϱ and T. Therefore, helium ignition can be delayed by axion cooling. This implies that the core grows more massive before helium ignites. One consequence is that the RGB will extend to brighter stars, i.e., the brightness of the brightest red giant in a given globular cluster signifies the core mass at helium ignition. Detailed studies reveal that the core mass at helium ignition agrees with theoretical expectations within 5–10% [10, 52, 53, 54, 55]. In turn, this implies that a novel energy-loss rate at $T = 10^8\,\mathrm{K}$ and an average density $\langle\varrho\rangle = 2 \times 10^5\,\mathrm{g\,cm^{-3}}$ should not exceed about $10\,\mathrm{erg\,g^{-1}\,s^{-1}}$. At these conditions the standard neutrino emission is about $4\,\mathrm{erg\,g^{-1}\,s^{-1}}$.

The helium-burning lifetime is useful to constrain the axion-photon interaction because the Primakoff rate is suppressed in the degenerate red-giant cores and thus is more effective in HB stars. The helium-ignition argument, on the other hand, is useful when the emission rate is larger on the RGB than on the HB as for bremsstrahlung $e + Ze \to Ze + e + a$. For the conditions in a red-giant core one finds $\varepsilon_{\mathrm{brems}} \approx \alpha_{aee}\, 2 \times 10^{27}\,\mathrm{erg\,g^{-1}\,s^{-1}}$ [54] so that

$$\alpha_{aee} < 0.5 \times 10^{-26} \quad \text{or} \quad g_{aee} < 3 \times 10^{-13}\,. \tag{3.19}$$

In the DFSZ model this limit corresponds to $f_a/\cos^2\beta > 0.8 \times 10^9\,\mathrm{GeV}$, $m_a < 9\,\mathrm{meV}/\cos^2\beta$, and $g_{a\gamma\gamma}\cos^2\beta < 1.2 \times 10^{-12}\,\mathrm{GeV}^{-1}$.

3.4.3 Asymptotic Giant Branch (AGB) Evolution

For axion-electron interactions near or even below the bound (3.19), the emission will strongly affect the evolutionary behavior of AGB stars [56]. However, these results have not been linked closely enough to observational data to obtain new limits or discover evidence for axion emission.

3.5 White-Dwarf Cooling

The degenerate core of a low-mass red giant before helium ignition is essentially a helium white dwarf. After the HB phase, when helium burning has ended, low-mass stars once more ascend the red-giant branch as "asymptotic giants" (AGB stars). They have a degenerate carbon-oxygen core and helium

burning in a shell. Fast mass loss creates a "planetary nebula" surrounding a compact remnant, a white dwarf, that first cools by neutrino emission and later by surface photon emission.

The observed white-dwarf luminosity function reveals that their cooling speed agrees with expectations, constraining new cooling agents such as axion emission [10, 57, 58, 59]. The resulting limit on the axion-electron coupling of $\alpha_{aee} \lesssim 1 \times 10^{-26}$ is comparable to the globular-cluster limit of (3.19).

The cooling speed of individual white dwarfs can be estimated in some cases where they appear as ZZ Ceti stars, i.e., when they are pulsationally unstable and when the period decrease $\dot{P}/P$ can be measured, a quantity that is sensitive to the cooling speed. A well-studied case is the star G117–B15A. For some time, it seemed to be cooling too fast, an effect that could have been attributed to axion cooling with $\alpha_{aee} = 0.2\text{–}0.8 \times 10^{-26}$ [60]. More recent analyses no longer require a new cooling channel, allowing one to set a limit on axion losses corresponding to[1] [61, 62]

$$\alpha_{aee} < 1.3 \times 10^{-27} \quad \text{or} \quad g_{aee} < 1.3 \times 10^{-13} \tag{3.20}$$

at a statistical 95% CL. In the DFSZ model this implies $m_a < 5\,\mathrm{meV}/\cos^2\beta$. This is the most restrictive limit on the axion-electron interaction.

3.6 Supernova 1987A

3.6.1 Energy-Loss Argument

About two dozen neutrinos from SN 1987A were observed about 20 years ago in several detectors [63]. The total number of events, their energies, and the distribution over several seconds correspond reasonably well to theoretical expectations. In the standard picture [64, 65], the core collapse of a massive star leads to a proto neutron star, a solar-mass object at nuclear density and temperature of several 10 MeV, where even neutrinos are trapped. The long time scale of emission is explained by diffusive neutrino energy transport. The emission of more weakly-interacting particles can be a more efficient energy-loss channel, resulting in a reduced neutrino burst duration. The late-time signal is most sensitive to such losses because the early neutrino emission is powered by accretion and thus not very sensitive to volume losses.

This argument has been applied to many cases, from right-handed neutrinos to Kaluza-Klein gravitons, but axions are the earliest and most widely discussed example [23, 66, 67, 68, 69, 70, 71, 72, 73, 74, 75]. They are emitted by nucleon bremsstrahlung $N + N \to N + N + a$ that depends on the axion-nucleon Yukawa coupling g_{aNN}, here taken to be an average of the

[1] The limit on g_{aee} stated in [61] is an order of magnitude more restrictive, but this is an obvious misprint. Likewise, their stated limit $m_a < 5\,\mathrm{meV}\,\cos^2\beta$ has an incorrect scaling with $\cos^2\beta$.

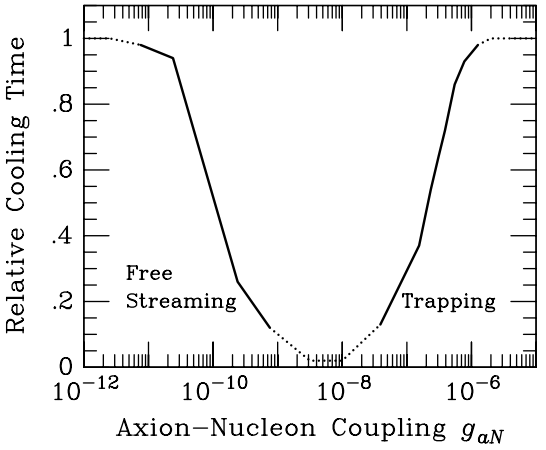

Fig. 3.2. Relative duration of a SN neutrino burst as a function of the axion-nucleon coupling [10]. Freely streaming axions are emitted from the entire core volume, trapped ones from an "axion sphere". The solid line is from numerical calculations [71, 72]. The dotted line is an arbitrary continuation to guide the eye

couplings to neutrons and protons. Figure 3.2 illustrates that axion emission leaves the signal duration unchanged when g_{aNN} is very small. For larger couplings, the signal is shortened until it reaches a minimum, roughly when the axion mfp corresponds to the geometric size of the SN core. For even larger couplings, axions are trapped and are emitted from an "axion sphere". When it moves beyond the neutrino sphere, the signal duration once more remains unaffected.

Of course, such "strongly" interacting axions are not necessarily harmless. They may play an important role during the infall phase. Moreover, in the water Cherenkov detectors that registered the SN 1987A neutrinos, these axions would have interacted with oxygen nuclei, leading to the release of γ rays and causing too many events [76].

However, for axions and other particles, the trapping regime is usually excluded by other arguments so that the free-streaming regime is of greater interest. An approximate analytic constraint on the energy-loss rate is [9]

$$\varepsilon_a \lesssim 1 \times 10^{19}\,\mathrm{erg\,g^{-1}\,s^{-1}}\,, \tag{3.21}$$

to be calculated at $\varrho = 3 \times 10^{14}\,\mathrm{g\,cm^{-3}}$ and $T = 30\,\mathrm{MeV}$. If we take the SN core to have a mass of about $1\,M_\odot = 2 \times 10^{33}\,\mathrm{g}$, this corresponds to an axion luminosity $L_a = \varepsilon_a M_\odot = 2 \times 10^{52}\,\mathrm{erg\,s^{-1}}$. The gravitational binding energy of the neutron star is about $3 \times 10^{53}\,\mathrm{erg}$ and the emission lasts up to 10 s, i.e., axion losses would compete significantly with neutrino emission.

We stress that the criterion (3.21) is not arbitrary, but was distilled from several numerical simulations that consistently showed that the burst duration was roughly halved when the limit (3.21) was saturated [9]. Axion losses

are then not small so that $T = 30\,\mathrm{MeV}$ is not the unperturbed temperature of these models. Different numerical models with different input physics probably have internal temperatures that are more similar once significant axion losses are included. In any event, (3.21) represents quite accurately the results from different simulations.

Recently, self-consistent cooling calculations were performed for Kaluza-Klein gravitons [77], once more confirming (3.21). The neutrino signal duration was directly compared with the data, and the limit, corresponding to (3.21), was found to have a 95% statistical CL.

Of course, this and any other numerical study rely on input physics for which systematic uncertainties are difficult to quantify, notably the nuclear equation of state and the neutrino opacities. In addition, the data are very sparse so that any conclusion based on them suffers from the usual problems of small-number statistics. Therefore, (3.21) should be viewed as a reasonable guide as to where a new energy-loss channel causes a significant tension with the SN 1987A pulse duration.

3.6.2 Axion Emission from a Nuclear Medium

In order to apply (3.21) to axions one needs the emission rate from a hot medium at nuclear density. The main emission process is nucleon bremsstrahlung, $N + N \to N + N + a$, but a reliable calculation of the rate is difficult. Axions couple to the nucleon spin so that bremsstrahlung requires the spin to "jiggle" in a collision, i.e., spin-conserving interactions do not contribute. This leaves the nuclear tensor force that is only crudely modeled by one-pion exchange (OPE). In a dense medium, other problems include the modification of particle masses and couplings as well as many-body and multiple-scattering effects.

One approach to estimate the emission rate relies on linear response theory where emission, absorption, and scattering of neutrinos, axions, and other particles depend only on a few "form factors" of the medium, i.e., the dynamical structure functions [73, 78, 79, 80, 81, 82, 83, 84, 85, 86]. This approach is perturbative to lowest order in the weak interaction between neutrinos (or axions) and nucleons, whereas the interactions among the medium constituents are lumped into the structure functions.

Assuming the medium to consist of one species of non-relativistic nucleons, the relevant quantity is the dynamical spin-density structure function [73]

$$S_\sigma(\omega,\mathbf{k}) = \frac{4}{3n_B}\int_{-\infty}^{+\infty} \mathrm{d}t\, \mathrm{e}^{\mathrm{i}\omega t}\, \langle \boldsymbol{\sigma}(t,\mathbf{k})\cdot\boldsymbol{\sigma}(0,-\mathbf{k})\rangle \ , \tag{3.22}$$

where n_B is the nucleon (baryon) density and $\boldsymbol{\sigma}(t,\mathbf{k})$ the spatial Fourier transform of the nucleon spin-density operator. The basic principles of quantum mechanics imply the detailed-balancing condition

$$S_\sigma(-\omega,\mathbf{k}) = S_\sigma(\omega,\mathbf{k})\,\mathrm{e}^{-\omega/T} \ . \tag{3.23}$$

The structure function obeys the sum rule

$$\int_{-\infty}^{+\infty} \frac{\mathrm{d}\omega}{2\pi}\, S_\sigma(\omega,\mathbf{k}) = 1 + \frac{4}{3n_B} \left\langle \sum_{\substack{i,j=1\\ i\neq j}}^{N_B} \mathbf{s}_i \cdot \mathbf{s}_j \, \cos(\mathbf{k}\cdot\mathbf{r}_{ij}) \right\rangle , \tag{3.24}$$

where $\mathbf{s}_i$ is the spin operator of nucleon i. The f-sum rule includes a factor ω under the integral and establishes a relation to the average nucleon-nucleon spin interaction energy [82]. It is often assumed that the higher sums $\int \mathrm{d}\omega\, \omega^n\, S(\omega,\mathbf{k})$ also exist for all n.

The axion absorption rate and the volume energy-loss rate are given in terms of the structure function as

$$\begin{aligned} \Gamma_a &= \left(\frac{C_N}{2f_a}\right)^2 \frac{n_B}{2}\, \omega\, S_\sigma(\omega,k) \,, \\ Q_a &= \left(\frac{C_N}{2f_a}\right)^2 \frac{n_B}{4\pi^2} \int_0^\infty \mathrm{d}\omega\, \omega^4\, S_\sigma(-\omega,k) \,, \end{aligned} \tag{3.25}$$

where $k = |\mathbf{k}| \approx \omega$ is the modulus of the axion momentum. Neutrino scattering, emission and absorption rates based on the axial vector current are given by similar phase-space integrals.

A reliable expression for $S_\sigma(\omega,k)$ is not available, so we need to use heuristic reasoning. The large nucleon mass compared to the emitted axion energy suggests the use of long-wavelength approximation $S_\sigma(\omega) = \lim_{\mathbf{k}\to 0} S_\sigma(\omega,\mathbf{k})$, i.e., we neglect the momentum transfer to the medium. In this limit (3.22) represents essentially the Fourier transform of the autocorrelation function of a single nucleon spin.

If we picture the nucleon spin as a classical vector that is kicked by a random force, we find [79]

$$S_\sigma^{\mathrm{class}}(\omega) = \frac{\Gamma_\sigma}{\omega^2 + \Gamma_\sigma^2/4} \,, \tag{3.26}$$

where Γ_σ is the spin fluctuation rate. Being a classical result, the quantum-mechanical detailed-balancing property is missing. Overall we thus write

$$S_\sigma(\omega) = \frac{\Gamma_\sigma}{\omega^2 + \Gamma_\sigma^2/4}\, s(\omega/T) \times \begin{cases} 1 & \text{for } \omega \geq 0, \\ \mathrm{e}^{\omega/T} & \text{for } \omega < 0, \end{cases} \tag{3.27}$$

where $s(x)$ is an even function normalized to $s(0) = 1$. The axion emission rate per unit mass, $\varepsilon_a = Q_a/\varrho$, therefore is

$$\varepsilon_a = \left(\frac{C_N}{2f_a}\right)^2 \frac{T^4}{\pi^2 m_N} F = 3.0\times 10^{37}\, \frac{\mathrm{erg}}{\mathrm{g\ s}}\, C_N^2 \left(\frac{\mathrm{GeV}}{f_a}\right)^2 \left(\frac{T}{30\,\mathrm{MeV}}\right)^4 F \,, \tag{3.28}$$

where

$$F = \int_0^\infty \mathrm{d}x \, \frac{x^4 \, \mathrm{e}^{-x}}{4} \, \frac{\Gamma_\sigma/T}{x^2 + (\Gamma_\sigma/2T)^2} \, s(x) \; . \tag{3.29}$$

For $\Gamma_\sigma/T \ll 1$ (dilute medium) assuming $s(x) = 1$, we find $F = \Gamma_\sigma/2T$.

A perturbative calculation, relevant for a dilute medium, using the OPE approximation yields [70, 79]

$$\Gamma_\sigma^{\rm OPE} = 4\pi^{1/2}\alpha_\pi^2 \, \frac{n_B T^{1/2}}{m_N^{5/2}} = 450\,\mathrm{MeV} \, \frac{\varrho}{3{\times}10^{14}\,\mathrm{g\,cm^{-3}}} \left(\frac{T}{30\,\mathrm{MeV}}\right)^{1/2} , \tag{3.30}$$

where $\alpha_\pi = (f 2m_N/m_\pi)^2/4\pi \approx 15$ with $f \approx 1.0$. For soft energies, bremsstrahlung depends only on the on-shell spin-dependent nucleon scattering rate. Based on measured nuclear phase shifts it was argued that the OPE result was an overestimation by about a factor of 4 [75].

Either way, Γ_σ/T is not small compared to unity, but also not very large. A possible range $1 \lesssim \Gamma_\sigma/T \lesssim 10$ appears generous. With $s(x) = 1$, this would imply $F \approx 0.5$ for $\Gamma_\sigma/T = 1$, a maximum of $F \approx 1.35$ near $\Gamma_\sigma/T = 7$ and $F \approx 1.3$ for $\Gamma_\sigma/T = 10$. Of course, $s(x)$ probably decreases with x or else the f-sum and higher sums of $S_\sigma(\omega)$ diverge. On the basis of existing information, one cannot do better than assume F to be a factor of order unity.

The SN 1987A limits are particularly interesting for hadronic axions where the bounds on α_{aee} are moot. Therefore, we use $C_p = -0.4$ and $C_n = 0$. Initially the proton fraction is relatively large so that we use $Y_p = 0.3$ to scale the emission rate to the proton density. With $F = 1$ and $T = 30\,\mathrm{MeV}$ we then find $\varepsilon_a = 1.4 \times 10^{36}\,\mathrm{erg\,g^{-1}\,s^{-1}}$ so that (3.21) implies

$$f_a \gtrsim 4 \times 10^8\,\mathrm{GeV} \qquad \text{and} \qquad m_a \lesssim 16\,\mathrm{meV} \; . \tag{3.31}$$

Despite a lot of effort that has gone into understanding the axion emission rate, these limits remain fairly rough estimates.

3.7 Conclusions

Astrophysics and cosmology provide the most restrictive limits on the axion hypothesis as summarized in Fig. 3.3. Beginning with cosmology, a cold axion population would emerge in the early universe that can make up the dark matter, but the required axion mass involves many uncertainties [87]. Galactic dark matter axions will be searched by the ADMX experiment in the mass range $m_a = 1$–$100\,\mu\mathrm{eV}$ [38, 88, 89, 90].

In addition, a population of hot axions is produced. Before confinement, the relevant processes involve quarks and gluons [91, 92]. Later the most generic process is $\pi + \pi \leftrightarrow \pi + a$ [93]. Axions decouple after the QCD epoch if $f_a \lesssim 3 \times 10^7\,\mathrm{GeV}$ ($m_a \gtrsim 0.2\,\mathrm{eV}$). Some of these hot dark-matter axions would be trapped in galaxies and galaxy clusters. An unsuccesful search for a decay

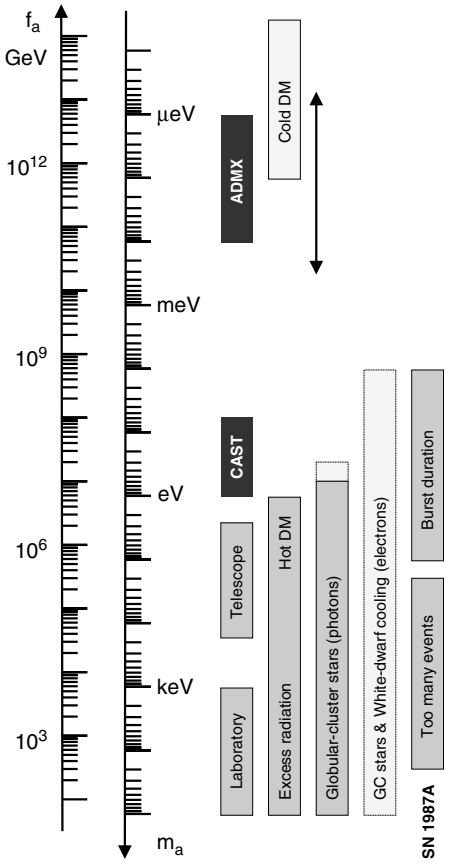

Fig. 3.3. Summary of astrophysical and cosmological axion limits as discussed in the text. The black sensitivity bars indicate the search ranges of the CAST solar axion search and the ADMX search for galactic dark matter axions. Light-grey exclusion bars are very model-dependent

line [94, 95, 96] provides direct limits on a range of axion masses marked "Telescope" in Fig. 3.3. Moreover, the usual structure-formation arguments provide the hot dark-matter limits [97, 98]. Axions decay on a cosmic time scale for $m_a \gtrsim 20\,\mathrm{eV}$. The decay photons would cause a variety of observable consequences [99], seamlessly connecting with the hot dark-matter limit so that cosmology alone rules out axions in the entire mass range $m_a > 1\,\mathrm{eV}$.

Figure 3.3 also shows the stellar-evolution limits discussed in this chapter, notably the globular-cluster limit on the axion-photon coupling. The globular-cluster and white-dwarf limits for DFSZ axions with $\cos^2\beta = 1$ are shown as a light-grey exclusion bar. Even in the DFSZ model, the axion-electron coupling could be accidentally small and at tree level it is entirely absent for

hadronic axions. Therefore, these limits are far less generic than those based on the axion-photon or axion-nucleon interaction.

The requirement that the neutrino signal of SN 1987A was not excessively shortened by axion losses pushes the limits down to $m_a \lesssim 10\,\mathrm{meV}$. However, this limit involves many uncertainties that are difficult to quantify, so it is somewhat schematic. The CAST search for solar axions [46] covers new territory in the parameter plane of m_a and $g_{a\gamma\gamma}$, but a signal would represent a conflict with the SN 1987A limit. While this limit certainly suggests that axions more plausibly have masses relevant for cold dark matter, a single argument, measurement, or observation is never conclusive.

In the DFSZ model, the limits from white-dwarf cooling based on the axion-electron interaction and those from SN 1987A from the axion-nucleon interaction are quite similar. Therefore, axion emission could still play an important role as an energy-loss channel of both SNe and white dwarfs and for other evolved stars, e.g. asymptotic giant stars.

In summary, axions provide a show-case example for the fascinating interplay between astrophysics, cosmology, and particle physics to solve some of the deepest mysteries at the interface between inner space and outer space.

Acknowledgments

Partial support by the Deutsche Forschungsgemeinschaft under grant SFB 375 and the European Union, contract RII3-CT-2004-506222 (ILIAS project), is acknowledged.

References

1. Gamow, G., Schoenberg, M.: The possible role of neutrinos in stellar evolution. Phys. Rev. **58**, 1117 (1940)
2. Gamow, G., Schoenberg, M.: Neutrino theory of stellar collapse. Phys. Rev. **59**, 539 (1941)
3. Bernstein, J., Ruderman, M., Feinberg, G.: Electromagnetic properties of the neutrino. Phys. Rev. **132**, 1227 (1963)
4. Stothers, R.B.: Astrophysical determination of the coupling constant for the electron-neutrino weak interaction. Phys. Rev. Lett. **24**, 538 (1970)
5. Sato, K., Sato, H.: Higgs meson emission from a star and a constraint on its mass. Prog. Theor. Phys. **54**, 1564 (1975)
6. Dicus, D.A., Kolb, E.W., Teplitz, V.L., Wagoner, R.V.: Astrophysical bounds on the masses of axions and Higgs particles. Phys. Rev. D **18**, 1829 (1978)
7. Vysotsky, M.I., Zeldovich, Y.B., Khlopov, M.Y., Chechetkin, V.M.: Some astrophysical limitations on the axion mass. Pisma Zh. Eksp. Teor. Fiz. **27**, 533 (1978) [JEPT Lett. **27**, 502 (1978)]
8. Turner, M.S.: Windows on the axion. Phys. Rept. **197**, 67 (1990)

9. Raffelt, G.G.: Astrophysical methods to constrain axions and other novel particle phenomena. Phys. Rept. **198**, 1 (1990)
10. Raffelt, G.G.: Stars as laboratories for fundamental physics. University of Chicago Press, Chicago (1996)
11. Raffelt, G.G.: Particle physics from stars. Ann. Rev. Nucl. Part. Sci. **49**, 163 (1999) [hep-ph/9903472]
12. Yao, W.M., et al.: (Particle Data Group), Review of particle physics. J. Phys. G **33**, 1 (2006)
13. Georgi, H., Kaplan, D.B., Randall, L.: Manifesting the invisible axion at low energies. Phys. Lett. B **169**, 73 (1986)
14. Kamionkowski, M., March-Russell, J.: Planck scale physics and the Peccei-Quinn mechanism. Phys. Lett. B **282**, 137 (1992) [hep-th/9202003]
15. Barr, S.M., Seckel, D.: Planck scale corrections to axion models. Phys. Rev. D **46**, 539 (1992)
16. Gasser, J., Leutwyler, H.: Quark masses. Phys. Rept. **87**, 77 (1982)
17. Leutwyler, H.: The ratios of the light quark masses. Phys. Lett. B **378**, 313 (1996) [hep-ph/9602366]
18. Kim, J.E.: Weak interaction singlet and strong CP invariance. Phys. Rev. Lett. **43**, 103 (1979)
19. Shifman, M.A., Vainshtein, A.I., Zakharov, V.I.: Can confinement ensure natural CP invariance of strong interactions?. Nucl. Phys. B **166**, 493 (1980)
20. Zhitnitsky, A.R.: On possible suppression of the axion hadron interactions. Sov. J. Nucl. Phys. **31**, 260 (1980) [Yad. Fiz. **31**, 497 (1980)]
21. Dine, M., Fischler, W., Srednicki, M.: A simple solution to the strong CP problem with a harmless axion. Phys. Lett. B **104**, 199 (1981)
22. Cheng, S.L., Geng, C.Q., Ni, W.T.: Axion-photon couplings in invisible axion models. Phys. Rev. D **52**, 3132 (1995) [hep-ph/9506295]
23. Raffelt, G., Seckel, D.: Bounds on exotic particle interactions from SN 1987A. Phys. Rev. Lett. **60**, 1793 (1988)
24. Carena, M., Peccei, R.D.: The effective Lagrangian for axion emission from SN 1987A. Phys. Rev. D **40**, 652 (1989)
25. Alexakhin, V.Y., et al. (COMPASS Collaboration): The deuteron spin-dependent structure function g_1^d and its first moment. Phys. Lett. B **647**, 8 (2007) [hep-ex/0609038]
26. Airapetian, A. (HERMES Collaboration): Precise determination of the spin structure function g_1 of the proton, deuteron and neutron. [hep-ex/0609039]
27. Ellis, J.R., Karliner, M.: The strange spin of the nucleon. In: Frois, B., Hughes, V.W., De Groot, N. (eds.) The Spin Structure of the Nucleon: International School of Nucleon Structure. Erice, Italy (3–10 August 1995) World Scientific, Singapore (1997) [hep-ph/9601280]
28. Primakoff, H.: Photo-production of neutral mesons in nuclear electric fields and the mean life of the neutral meson. Phys. Rev. **81**, 899 (1951)
29. Raffelt, G.G.: Astrophysical axion bounds diminished by screening effects. Phys. Rev. D **33**, 897 (1986)
30. Altherr, T., Petitgirard, E., del Río Gaztelurrutia, T.: Axion emission from red giants and white dwarfs. Astropart. Phys. **2**, 175 (1994) [hep-ph/9310304]
31. Raffelt, G.G.: Plasmon decay into low mass bosons in stars. Phys. Rev. D **37**, 1356 (1988)

32. Zavattini, E., et al. (PVLAS Collaboration): Experimental observation of optical rotation generated in vacuum by a magnetic field. Phys. Rev. Lett. **96**, 110406 (2006) [hep-ex/0507107]
33. Cameron, R., et al.: Search for nearly massless, weakly coupled particles by optical techniques. Phys. Rev. D **47**, 3707 (1993)
34. Schlattl, H., Weiss, A., Raffelt, G.: Helioseismological constraint on solar axion emission. Astropart. Phys. **10**, 353 (1999) [hep-ph/9807476]
35. Bahcall, J.N., Serenelli, A.M., Basu, S.: New solar opacities, abundances, helioseismology, and neutrino fluxes. Astrophys. J. **621**, L85 (2005) [astro-ph/0412440]
36. Ahmad, Q.R., et al. (SNO Collaboration): Direct evidence for neutrino flavor transformation from neutral-current interactions in the Sudbury Neutrino Observatory. Phys. Rev. Lett. **89**, 011301 (2002) [nucl-ex/0204008]
37. Aharmim, B., et al. (SNO Collaboration): Electron energy spectra, fluxes, and day-night asymmetries of B-8 solar neutrinos from the 391-day salt phase SNO data set. Phys. Rev. C **72**, 055502 (2005) [nucl-ex/0502021]
38. Sikivie, P.: Experimental tests of the invisible axion. Phys. Rev. Lett. **51**, 1415 (1983); (E) ibid. **52**, 695 (1984)
39. Raffelt, G., Stodolsky, L.: Mixing of the photon with low mass particles. Phys. Rev. D **37**, 1237 (1988)
40. Lazarus, D.M., Smith, G.C., Cameron, R., Melissinos, A.C., Ruoso, G., Semertzidis, Y.K., Nezrick, F.A.: A search for solar axions. Phys. Rev. Lett. **69**, 2333 (1992)
41. Moriyama, S., Minowa, M., Namba, T., Inoue, Y., Takasu, Y., Yamamoto, A.: Direct search for solar axions by using strong magnetic field and x-ray detectors. Phys. Lett. B **434**, 147 (1998) [hep-ex/9805026]
42. Inoue, Y., Namba, T., Moriyama, S., Minowa, M., Takasu, Y., Horiuchi, T., Yamamoto, A.: Search for sub-electronvolt solar axions using coherent conversion of axions into photons in magnetic field and gas helium. Phys. Lett. B **536**, 18 (2002) [astro-ph/0204388]
43. Avignone, F.T., et al. (SOLAX Collaboration): Experimental search for solar axions via coherent Primakoff conversion in a germanium spectrometer. Phys. Rev. Lett. **81**, 5068 (1998) [astro-ph/9708008]
44. Morales, A., et al. (COSME Collaboration): Particle dark matter and solar axion searches with a small germanium detector at the Canfranc underground laboratory. Astropart. Phys. **16**, 325 (2002) [hep-ex/0101037]
45. Bernabei, R., et al.: Search for solar axions by Primakoff effect in NaI crystals. Phys. Lett. B **515**, 6 (2001)
46. Zioutas, K., et al. (CAST Collaboration): First results from the CERN axion solar telescope (CAST). Phys. Rev. Lett. **94**, 121301 (2005) [hep-ex/0411033]
47. van Bibber, K., McIntyre, P.M., Morris, D.E., Raffelt, G.G.: A practical laboratory detector for solar axions. Phys. Rev. D **39**, 2089 (1989)
48. Raffelt, G.G., Starkman, G.D.: Stellar energy transfer by keV mass scalars. Phys. Rev. D **40**, 942 (1989)
49. Buzzoni, A., Fusi Pecci, F., Buonanno, R., Corsi, C.E.: Helium abundance in globular clusters: the R-method. Astron. Astrophys. **128**, 94 (1983)
50. Buonanno, R., Buzzoni, A., Corsi, C.E., Fusi Pecci, F., Sandage, A.R.: High precision photometry of 10000 stars in M3. Mem. Soc. Astron. Ital. **57**, 391 (1986)

51. Renzini, A., Fusi Pecci, F.: Tests of evolutionary sequences using color-magnitude diagrams of globular clusters. Annu. Rev. Astron. Astrophys. **26**, 199 (1988)
52. Raffelt, G.G.: Core mass at the helium flash from observations and a new bound on neutrino electromagnetic properties. Astrophys. J. **365**, 559 (1990)
53. Raffelt, G.G.: New bound on neutrino dipole moments from globular cluster stars. Phys. Rev. Lett. **64**, 2856 (1990)
54. Raffelt, G., Weiss, A.: Red giant bound on the axion-electron coupling revisited. Phys. Rev. D **51**, 1495 (1995) [hep-ph/9410205]
55. Catelan, M., de Freitas Pacheco, J.A., Horvath, J.E.: The helium-core mass at the helium flash in low-mass red giant stars: Observations and theory. Astrophys. J. **461**, 231 (1996) [astro-ph/9509062]
56. Domínguez, I., Straniero, O., Isern, J.: Asymptotic giant branch stars as astroparticle laboratories. Mon. Not. R. Astron. Soc. **306**, L1 (1999) [astro-ph/9905033]
57. Raffelt, G.G.: Axion constraints from white dwarf cooling times. Phys. Lett. B **166**, 402 (1986)
58. Wang, J.: Constraints of axions from white dwarf cooling. Mod. Phys. Lett. A **7**, 1497 (1992)
59. Blinnikov, S.I., Dunina-Barkovskaya, N.V.: The cooling of hot white dwarfs: A theory with non-standard weak interactions and a comparison with observations. Mon. Not. R. Astron. Soc. **266**, 289 (1994)
60. Isern, J., Hernanz, M., García-Berro, E.: Axion cooling of white dwarfs. Astrophys. J. **392**, L23 (1992)
61. Córsico, A.H., Benvenuto, O.G., Althaus, L.G., Isern, J., García-Berro, E.: The potential of the variable DA white dwarf G117-B15A as a tool for fundamental physics. New Astron. **6**, 197 (2001) [astro-ph/0104103]
62. Isern, J., García-Berro, E.: White dwarf stars as particle physics laboratories. Nucl. Phys. Proc. Suppl. **114**, 107 (2003)
63. Koshiba, M.: Observational neutrino astrophysics. Phys. Rept. **220**, 229 (1992)
64. Burrows, A.: Supernova explosions in the universe. Nature **403**, 727 (2000)
65. Woosley, S., Janka, T.: The physics of core-collapse supernovae. Nature Physics **1**, 147 (2005) [astro-ph/0601261]
66. Ellis, J.R., Olive, K.A.: Constraints on light particles from supernova 1987A. Phys. Lett. B **193**, 525 (1987)
67. Turner, M.S.: Axions from SN 1987A. Phys. Rev. Lett. **60**, 1797 (1988)
68. Mayle, R., Wilson, J.R., Ellis, J.R., Olive, K.A., Schramm, D.N., Steigman, G.: Constraints on axions from SN 1987A. Phys. Lett. B **203**, 188 (1988)
69. Mayle, R., Wilson, J.R., Ellis, J.R., Olive, K.A., Schramm, D.N., Steigman, G.: Updated constraints on axions from SN 1987A. Phys. Lett. B **219**, 515 (1989)
70. Brinkmann, R.P., Turner, M.S.: Numerical rates for nucleon-nucleon axion bremsstrahlung. Phys. Rev. D **38**, 2338 (1988)
71. Burrows, A., Turner, M.S., Brinkmann, R.P.: Axions and SN 1987A. Phys. Rev. D **39**, 1020 (1989)
72. Burrows, A., Ressell, M.T., Turner, M.S.: Axions and SN 1987A: Axion trapping. Phys. Rev. D **42**, 3297 (1990)
73. Janka, H.T., Keil, W., Raffelt, G., Seckel, D.: Nucleon spin fluctuations and the supernova emission of neutrinos and axions. Phys. Rev. Lett. **76**, 2621 (1996) [astro-ph/9507023]

74. Keil, W., Janka, H.T., Schramm, D.N., Sigl, G., Turner, M.S., Ellis, J.R.: A fresh look at axions and SN 1987A. Phys. Rev. D **56**, 2419 (1997) [astro-ph/9612222]
75. Hanhart, C., Phillips, D.R., Reddy, S.: Neutrino and axion emissivities of neutron stars from nucleon nucleon scattering data. Phys. Lett. B **499**, 9 (2001) [astro-ph/0003445]
76. Engel, J., Seckel, D., Hayes, A.C.: Emission and detectability of hadronic axions from SN 1987A. Phys. Rev. Lett. **65**, 960 (1990)
77. Hanhart, C., Pons, J.A., Phillips, D.R., Reddy, S.: The likelihood of GODs' existence: Improving the SN 1987A constraint on the size of large compact dimensions. Phys. Lett. B **509**, 1 (2001) [astro-ph/0102063]
78. Raffelt, G., Seckel, D.: Multiple scattering suppression of the bremsstrahlung emission of neutrinos and axions in supernovae. Phys. Rev. Lett. **67**, 2605 (1991)
79. Raffelt, G., Seckel, D.: A selfconsistent approach to neutral current processes in supernova cores. Phys. Rev. D **52**, 1780 (1995) [astro-ph/9312019]
80. Raffelt, G., Seckel, D., Sigl, G.: Supernova neutrino scattering rates reduced by nucleon spin fluctuations: Perturbative limit. Phys. Rev. D **54**, 2784 (1996) [astro-ph/9603044]
81. Raffelt, G., Strobel, T.: Reduction of weak interaction rates in neutron stars by nucleon spin fluctuations: Degenerate case. Phys. Rev. D **55**, 523 (1997) [astro-ph/9610193]
82. Sigl, G.: Weak interactions in supernova cores and saturation of nucleon spin fluctuations. Phys. Rev. Lett. **76**, 2625 (1996) [astro-ph/9508046]
83. Raffelt, G., Sigl, G.: Numerical toy-model calculation of the nucleon spin autocorrelation function in a supernova core. Phys. Rev. D **60**, 023001 (1999) [hep-ph/9808476]
84. Yamada, S.: Reduction of neutrino nucleon scattering rate by nucleon nucleon collisions. Nucl. Phys. A **662**, 219 (2000) [astro-ph/9907045]
85. Sedrakian, A., Dieperink, A.E.L.: Coherent neutrino radiation in supernovae at two loops. Phys. Rev. D **62**, 083002 (2000) [astro-ph/0002228]
86. van Dalen, E.N.E., Dieperink, A.E.L., Tjon, J.A.: Neutrino emission in neutron stars. Phys. Rev. C 67, 065807 (2003) [nucl-th/0303037]
87. Sikivie, P.: Axion cosmology. In: Kuster M., Raffelt G., Beltrán B., (eds.) Lecture Notes in Physics, Vol. 741, pp. 51–71. Springer, Heidelberg (2008) [astro-ph/0610440]
88. Bradley, R., et al.: Microwave cavity searches for dark-matter axions. Rev. Mod. Phys. **75**, 777 (2003)
89. Asztalos, S.J., et al.: An improved RF cavity search for halo axions. Phys. Rev. D **69**, 011101 (2004) [astro-ph/0310042]
90. Duffy, L.D., et al.: A high resolution search for dark-matter axions. Phys. Rev. D **74**, 012006 (2006) [astro-ph/0603108]
91. Turner, M.S.: Thermal production of not so invisible axions in the early universe. Phys. Rev. Lett. **59**, 2489 (1987); (E) ibid. **60**, 1101 (1988)
92. Massó, E., Rota, F., Zsembinszki, G.: On axion thermalization in the early universe. Phys. Rev. D **66**, 023004 (2002) [hep-ph/0203221]
93. Chang, S., Choi, K.: Hadronic axion window and the big bang nucleosynthesis. Phys. Lett. B **316**, 51 (1993) [hep-ph/9306216]
94. Bershady, M.A., Ressell, M.T., Turner, M.S.: Telescope search for multi-eV axions. Phys. Rev. Lett. **66**, 1398 (1991)

95. Ressell, M.T.: Limits to the radiative decay of the axion. Phys. Rev. D **44**, 3001 (1991)
96. Grin, D., Covone, G., Kneib, J.P., Kamionkowski, M., Blain, A., Jullo, E.: A telescope search for decaying relic axions. Phys. Rev. D **75**, 105018 (2007) [astro-ph/0611502]
97. Hannestad, S., Raffelt, G.: Cosmological mass limits on neutrinos, axions, and other light particles. JCAP 0404, 008 (2004) [hep-ph/0312154]
98. Hannestad, S., Mirizzi, A., Raffelt, G.: New cosmological mass limit on thermal relic axions. JCAP 0507, 002 (2005) [hep-ph/0504059]
99. Massó, E., Toldra, R.: New constraints on a light spinless particle coupled to photons. Phys. Rev. D **55**, 7967 (1997) [hep-ph/9702275]